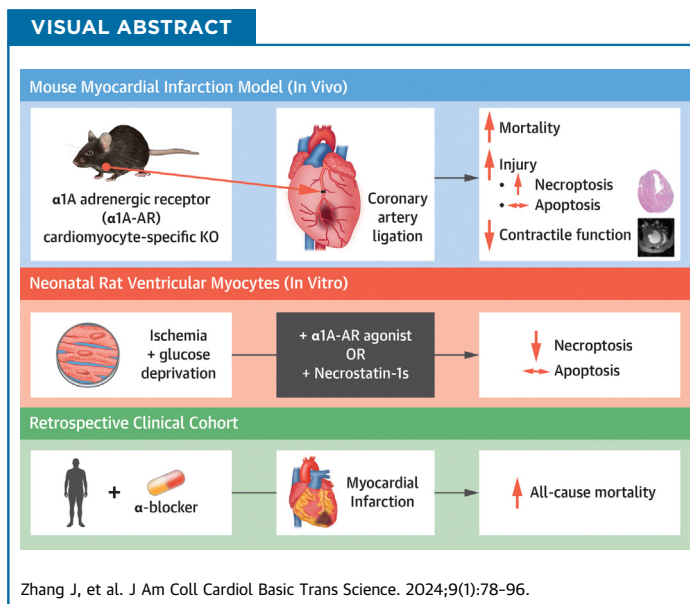**ORIGINAL RESEARCH - PRECLINICAL**

Cardiomyocyte Alpha-1A Adrenergic Receptors Mitigate Postinfarct Remodeling and Mortality by Constraining Necroptosis

Jiandong Zhang, MD, PhD,[a,b] Peyton B. Sandroni, BS,[b,c] Wei Huang, MS,[b] Xiaohua Gao, PhD,[d] Leah Oswalt, PhD,[b] Melissa A. Schroder, BS,[b] SungHo Lee, DVM, PhD,[e] Yen-Yu I. Shih, PhD,[e] Hsiao-Ying S. Huang, PhD,[f] Philip M. Swigart, MS,[c,g] Bat E. Myagmar, MD, PhD,[c,g] Paul C. Simpson, MD,[c,g] Joseph S. Rossi, MD,[a] Jonathan C. Schisler, PhD,[b,h] Brian C. Jensen, MD[a,b,h]

VISUAL ABSTRACT

Zhang J, et al. J Am Coll Cardiol Basic Trans Science. 2024;9(1):78-96.

HIGHLIGHTS

- Our study, the first to expose a cardiomyocyte-specific knockout of the α1A-AR subtype to injury, shows that the loss of cardiomyocyte α1A-ARs is associated with markedly increased mortality after myocardial infarction.

- Cardiomyocyte α1A-ARs protect against ischemic injury by constraining necroptosis.

- In our single-center clinical study, the use of α-blockers increased risk of mortality after MI, the first demonstration that these commonly used drugs may impact survival in high-risk patients.

From the [a]Division of Cardiology, University of North Carolina School of Medicine, Chapel Hill, North Carolina, USA; [b]UNC McAllister Heart Institute, University of North Carolina School of Medicine, Chapel Hill, North Carolina, USA; [c]Department of Medicine, University of California-San Francisco, San Francisco, California, USA; [d]Department of Epidemiology, University of North Carolina Gillings School of Public Health, Chapel Hill, North Carolina, USA; [e]Center for Animal MRI, University of North Carolina, Chapel Hill, North Carolina, USA; [f]Mechanical and Aerospace Engineering Department, North Carolina State University, Raleigh, North Carolina, USA; [g]San Francisco VA Medical Center, San Francisco, California, USA; and the [h]Department of Pharmacology, University of North Carolina, Chapel Hill, North Carolina, USA.

The authors attest they are in compliance with human studies committees and animal welfare regulations of the authors' institutions and Food and Drug Administration guidelines, including patient consent where appropriate. For more information, visit the Author Center.

SUMMARY

Clinical studies have shown that α1-adrenergic receptor antagonists (α-blockers) are associated with increased heart failure risk. The mechanism underlying that hazard and whether it arises from direct inhibition of cardiomyocyte α1-ARs or from systemic effects remain unclear. To address these issues, we created a mouse with cardiomyocyte-specific deletion of the α1A-AR subtype and found that it experienced 70% mortality within 7 days of myocardial infarction driven, in part, by excessive activation of necroptosis. We also found that patients taking α-blockers at our center were at increased risk of death after myocardial infarction, providing clinical correlation for our translational animal models. (J Am Coll Cardiol Basic Trans Science 2024;9:78–96)

ABBREVIATIONS AND ACRONYMS

α1A-AR = α-1A adrenergic receptor

cmAKO = cardiomyocyte-specific α-1A adrenergic receptor knockout mouse

HF = heart failure

LCA = left coronary artery

LV = left ventricle

MI = myocardial infarction

MLKL = mixed lineage kinase domain-like protein

RIP kinase = receptor-interacting protein kinase

WT = wild type

Despite significant advances in clinical management, acute myocardial infarction (MI) remains a leading source of morbidity and mortality worldwide and the number of patients who develop heart failure (HF) after MI is increasing.[1,2] Acute and subacute cardiomyocyte death are central to the pathobiology of MI and collectively determine the extent of post-infarct remodeling and the likelihood of consequent HF. Historically, cell death in the setting of MI has been attributed largely to passive necrosis and apoptosis, but there is increasing recognition that programmed necrosis (necroptosis) contributes meaningfully to post-infarct injury and remodeling.[3]

Activation of the sympathetic nervous system is well-established as a critical component of the physiological response to MI in both experimental animal models and humans.[4-6] Sympathetic nervous system activation is mediated by increased levels of the catecholamines norepinephrine (NE) and epinephrine that regulate their critical functions through binding to 2 major categories of adrenergic receptors (ARs) in the heart, alpha1-adrenergic receptors (α1-ARs) and beta-adrenergic receptor (β-ARs). Sustained hyperactivation of β1-ARs is a toxic driving force contributing to excessive cardiomyocyte death after MI and β-blockers have long been recognized as cornerstones of medical therapy in the immediate post-MI period.[7] The potential roles of cardiomyocyte α1-ARs in this context have received considerably less attention, but a growing body of experimental data indicates that α1-ARs protect against myocardial ischemic injury (reviewed in Jensen et al[8] and O'Connell et al[9]).

There are three subtypes of α1-ARs with distinct tissue distribution and physiological function in the heart. The α1A and α1B are the predominant α1-AR subtypes in rodent and human myocardium, whereas the α1D is found in coronary arterial smooth muscle.[10-13] Work published in the 1990s showed that nonselective α1-AR activation conferred protection against ischemia-reperfusion injury and limited post-infarct remodeling.[14,15] Subsequent studies have identified α1A as the cardioprotective α1-AR subtype in the context of both ischemic and nonischemic insults (reviewed in Zhang et al).[16] Overexpression of the α1A in mice and rats limits infarct size and protects contractile function after MI.[17,18] Global α1A knockout mice exhibit exacerbated post-infarct remodeling and apoptosis 4 weeks after left coronary artery (LCA) ligation, but the response to injury has not been studied in mice with cardiomyocyte-specific α1A deletion.[19]

Here, we have used Cre-lox breeding to develop a cardiomyocyte-specific α1A knockout (cmAKO) mouse line, obviating valid concerns about potential physiological confounding in global α1-AR loss-of-function models. We find that cmAKO mice experience markedly increased 1-week mortality after MI due to permanent LCA ligation, with evidence of exaggerated ventricular remodeling by day 3. In vivo and in vitro studies show enhanced activation of receptor-interacting protein (RIP) kinase-dependent necroptosis pathways in cmAKO mice, revealing a novel mechanism for α1A-mediated cardioprotection. We also show that male patients who were taking medications that block α1A-AR signaling at the time of percutaneous coronary intervention (PCI) for MI experienced a higher risk of mortality during a 5-year follow-up period, providing clinical correlation for our experimental findings.

METHODS

MICE. C57BL/6J and ROSA^mT/mG (stock # 007676) mice were purchased from Jackson lab. The cmAKO mouse line was generated by breeding *Myh6*-Cre (originally from the lab of E. Dale Abel at the University of Iowa and provided by Leslie Leinwand at the University of Colorado) to *Adra1a* flox/flox mice

with loxP sites flanking the first coding exon (constructed in the Paul C. Simpson lab at the University of California-San Francisco/San Francisco VA Medical Center).[20,21] All mice were backcrossed regularly and maintained on a C57BL/6 genetic background. Twelve- to 16-week-old males were used in all experiments. Floxed mice (αMHC-Cre[neg]/α1A^{fl/fl}) were used as wild-type (WT) controls for cmAKO mice.

ADULT MOUSE VENTRICULAR MYOCYTE ISOLATION AND CULTURE. Adult mouse ventricular myocytes (AMVMs) were isolated as described previously.[22] WT and knockout (KO) mice had deep anesthesia with isoflurane 3% in oxygen 0.5 to 1 L/min and intraperitoneal injection of heparin 0.5 mL 100 IU/mL in phosphate-buffered saline (PBS) to prevent coagulation of blood in the coronary arteries. The heart was removed by cutting the transverse aorta between the carotid arteries, and placed in a 60-mm dish at room temperature containing 10 mL of perfusion buffer (PB): Na-HEPES-buffered calcium-free solution containing (mmol/L) NaCl 120.4, KCl 14.7, KH2PO4 0.6, Na2HPO4 0.6, MgSO4-7H2O 1.2, Na-HEPES 10, NaHCO3 4.6, taurine 30, 2,3-butanedione monoxime 10, and glucose 5.5 (all from Sigma-Aldrich, except Na-HEPES, which was from Gibco BRL). After thymus and lungs were trimmed off, the heart was cannulated rapidly onto a Langendorff perfusion apparatus and perfused for 4 minutes at 3 mL/min to flush blood from the vasculature. The heart was then digested for 2 minutes at 3 mL/min with PB supplemented with collagenase II 2.4 mg/mL (Worthington Biochemical) without additional calcium, then for 8 minutes at 3 mL/min with PB with collagenase with additional CaCl2 40 μmol/L. A 50-mL digestion solution was prepared fresh for each heart and added to the reservoir just before digestion to prevent heat inactivation of the enzyme. The digested heart was transferred to a 60-mm dish containing 10 mL stop buffer (PB with 12.5 μmol/L CaCl2 and calf serum 10% to inactivate proteases [HyClone Defined Bovine Calf Serum SH30073]). After atria and large vessels were removed, ventricular tissue was disrupted and dissociated by mincing into ~10 to 15 small pieces using fine tip forceps, then triturating sequentially (~10 to 15 times each) through plastic pipettes with 3 mm, 2 mm, and 1 mm openings. After a 200 μL aliquot was obtained to count cells, the whole cell suspension was centrifuged for 2 minutes at 50*g* (Eppendorf Centrifuge 5804), the supernatant was removed, and the pellet was used in radioligand binding.

RADIOLIGAND BINDING. Isolated AMVMs were counted, pelleted, and suspended in Tris 50 mmol/L

pH 7.4 and EDTA 1 mmol/L. Cells were lysed using an ultrasonicator #W-380 (Heat Systems Ultrasonics) set at 50% duty cycle, output control 4 with 5x 5 second burst on ice. Cell numbers were set to 225,000 myocytes/mL. α1A-AR abundance was quantified by competition for binding of 3H-prazosin (0.5 nmol/L) with 22 concentrations (0.05 to 500 μmol/L) in duplicate of 5-methylurapidil (#U101, Sigma-Aldrich), an α1A-selective antagonist. Bound ligand was separated from free ligand by filtration with ice-cold assay buffer through glass fiber filters, rinsed 4 times with 4 mL cold assay buffer, dried, and counted.[23] Total receptor number and binding affinity (Kd) were calculated by nonlinear regression with Graph-Pad Prism.

QUANTITATIVE REVERSE TRANSCRIPTASE POLYMERASE CHAIN REACTION. Total RNA was isolated from cells and tissue (Qiagen RNeasy Plus mini kit #74134) and analyzed using a NanoDrop (ThermoScientific). For quantitative reverse transcriptase polymerase chain reaction (qRT-PCR), 1 μg of RNA was reverse transcribed using High Capacity cDNA Reverse Transcription Kit (Life Technologies #4368814). Two step qRT-PCR reactions contained 2% of the cDNA product. All reactions were performed in triplicate in a Roche 480 Light Cycler. Relative quantitation of polymerase chain reaction products used the ΔΔCt method relative to 2 validated reference genes (*Tbp* and *Polr2a*). Similar efficiencies were confirmed for all primers. All probes and primers were from Roche. Primer sequences included the following:

Tbp F:ggcggtttggctaggttt; R:gggttatcttcacacaccatga; UPL Probe # 107

Polr2a F:aatccgcatcatgaacagtg, R:tcatcatccattttatccacca; UPL Probe # 69

Adra1a F: attgtggtgggatgcttcgtcct; R: tgtttccggtggcttgaaattcgg; UPL Probe # 105

Adra1b F: ttcttcatcgctctcccact; R: gggttgaggcagctgttg; UPL Probe # 20

ECHOCARDIOGRAPHY. Transthoracic echocardiography was performed on conscious, loosely restrained mice in the McAllister Heart Institute Rodent Surgical Core using a VisualSonics Vevo 2100 ultrasound system (VisualSonics, Inc). Two-dimensional and M-mode echocardiography were performed in the parasternal long-axis view at the level of the papillary muscle. Left ventricular systolic function was assessed by fractional shortening (%FS = [(LVEDD − LVESD)/LVEDD] × 100, where *LVEDD* is left ventricular end-diastolic diameter and *LVESD* is left ventricular end-systolic diameter). Reported values represent the average of at least 5 cardiac cycles per mouse. Sonographers and investigators were blinded

to mouse treatment condition during image acquisition and analysis.

MOUSE MI MODEL. Mice were subjected to permanent LCA ligation as previously described and subsequently assessed for left ventricular (LV) morphology and function.[24] For LCA ligation as well as cardiectomy, mice were anesthetized by inhalation of isoflurane (2%). For postoperative analgesia, 5 mg meloxicam/kg body weight was applied every 24 hours for the first 72 hours post-surgery. For the Nec-1s (7-Cl-O-Nec-1, Sigma) studies, vehicle or Nec-1s (1.65 mg/kg body weight) was given intravenously 10 minutes before LCA ligation, followed by daily intravenous injections for 2 days.

IMMUNOSTAINING AND HISTOLOGICAL ANALYSIS. To fix heart tissue for immunohistochemistry, mice were heparinized and the heart was perfused with 10 mL of PBS followed by 20 mL of 4% paraformaldehyde (PFA)-PBS through a 23-gauge butterfly needle, then excised and placed in 4% PFA-PBS for 24 hours before transfer to 70% ethanol. Hearts were sectioned and stained using standard methods in the University of North Carolina Histology Research Core. Slides were scanned using an Aperio ScanScope (Aperio Technologies) and analyzed in Aperio ImageScope software. For immunohistochemistry, hearts were fixed overnight in 4% PFA-PBS, incubated in 30% sucrose–PBS, and then frozen in OTC medium (Tissue-Tek). Frozen sections (10 μm) obtained with a Leica cryostat (Leica) were placed on glass slides, dried at room temperature, and then incubated with primary antibodies (c-caspase-3, RIP kinase). After washing, sections were incubated for 3 hours at room temperature with secondary antibodies (1:1,000, Life Technologies). Terminal deoxynucleotidyl transferase dUTP nick end labeling staining used a horseradish peroxidase-diaminobenzidine (HRP-DAB) kit from Abcam (ab206386). Fluorescence was observed with a Zeiss LSM710 confocal microscope.

HISTOPATHOLOGICAL MEASUREMENT OF INFARCT SIZE. Infarct size was measured as previously described and 6 to 8 mouse hearts in each group were used for analysis.[25] Briefly, each LV was sliced in the transverse axis from the apex to the base using a microtome at 5-μm thickness with an interval of 300 μm between each section. All sections were mounted on glass slides and stained with hematoxylin and eosin for further quantitative analysis. Slides were scanned using an Aperio ScanScope (Aperio Technologies) and analyzed in Aperio ImageScope software. ImageJ software was used to measure areas of affected (infarction and infiltration) and whole LV myocardium. The affected area and the total area of LV myocardium were traced manually in the digital images by an investigator who was blinded to the genotype of the sample, then measured automatically by the computer. Infarct size as expressed as a percentage of total LV myocardial surface area was calculated by dividing the sum of injured areas from all sections by the sum of LV areas from all sections (including those without infarct) and multiplying by 100%.

CARDIAC MAGNETIC RESONANCE IMAGING. Anesthesia was induced by using 3% isoflurane followed by ≤2% isoflurane for maintenance as required. Respiration rate was used to monitor depth of anesthesia and was maintained between 20 and 70 breaths/min. Body temperature was monitored and controlled within the range of 37 ± 2 °C. Cardiac magnetic resonance imaging (MRI) gated to electrocardiogram was obtained in prone position using a 9 Tesla magnet equipped with a 370-mT/m gradient system, a 38-mm birdcage quadrature coil, and ParaVision 6.0 software. To assess cardiac function, short-axis images were acquired with the retrospectively-gated fast low angle shot sequence with the following settings: 7-9 slices; field-of-view: $4.5 \times 4.5 \times 0.1$ cm; image matrix size: 256×256; repetitions: 100; flip angle: 15°; echo time: 2.05 ms; repetition time: 8.91ms; number of reconstructed frames: 8. A single person contoured the ventricles, while a second person checked the quality of the contouring. In case of disagreement, the contouring was adjusted to achieve mutual agreement. End-systolic volume (ESV) and end-diastolic volume (EDV) cardiac phases were automatically determined for quality check of the cardiac contouring. A maximum mass difference of the left ventricle of 10% was allowed between both cardiac phases. The heart rate was extracted from the IntraGate sequence. These parameters were used to calculate the stroke volume ($SV = EDV - ESV$), cardiac output ($CO = SV \times$ heart rate) and ejection fraction ($EF = SV/EDV \times 100$). All measurements and calculations were made by investigators blinded to genotype.

MECHANICAL TESTING OF VENTRICULAR MYOCARDIUM. Mechanical testing was performed using a Biotester-5000 biaxial test system (Cellscale) following a previously reported method.[26] In brief, at day 3 post-MI, male mice were sacrificed. The LV was separated from the right ventricle and atria, and then cut in half along the long axis, creating a "sheet" of ventricular tissue. The isolated tissue was mounted biaxially on the Biotester with the infarct centered, then stretched according to manufacturer's protocols.[26] Deformation

was measured by image tracking analysis. Stresses and corresponding strains were fit to a 4-parameter Fung-type model where the strain energy density was calculated to yield the Cauchy stress. Tissue stiffness was quantified as the slope of the Cauchy stress-stretch ratio curve.

SERUM HMGB1 ENZYME-LINKED IMMUNOSORBENT ASSAY. Blood was obtained from the inferior vena cava at the time of sacrifice 3 days after LCA ligation. Detection of serum high-mobility group box 1 (HMGB1) was performed using a commercially available kit (Novus Biologicals).

IMMUNOBLOTTING. After sacrifice, the heart was quickly excised and sliced into 5 to 8 1.0-mm thick sections perpendicular to the long axis of the ventricular chambers. The infarct border zone was visualized under a dissecting microscope and dissected out. The border zone was defined as a rim of approximately 2 mm of tissue bordering the infarction. Visually apparent scar tissue was excised and discarded during the dissection process leaving only viable myocardial tissue for immunoblotting and further analysis. The tissue from the border zone was immediately placed into a cryovial, snap-frozen in liquid nitrogen, and stored at ‾80 °C. Samples were not pooled and 20 mg frozen heart tissue was used for immunoblotting of individual heart samples. Tissue and cell lysates were produced in radio-immunoprecipation assay buffer supplemented with PhosSTOP (Roche Diagnostics) and protease inhibitor cocktail (Roche Diagnostics). Subsequently, samples were incubated in $4 \times$ lithium dodecyl sulfate sample buffer, including 2% β-mercaptoethanol, for 10 minutes at 70 °C. Sodium dodecyl sulfate polyacrylamide gel electrophoresis and immunoblot analysis were performed using the 4% to 12% Nupage gel system (Life Technology) after balancing for protein content using a bicinchoninic acid assay. Membranes were blocked in 5% milk-Tris-buffered saline-Tween 20 and incubated in primary antibody overnight at 4 °C and then secondary HRP-conjugated antibodies for 1 hour at room temperature. Images were generated using Amersham ECL Select Western Blotting Detection Reagent (GE Healthcare Life Sciences) and the ChemiDoc Imaging System (Biorad).

ANTIBODIES. Antibodies used included: PARP/cleaved PARP Cell Signaling 9542, CAMKIId Abcam #181052, pCAMKIId Abcam #ab32678, RIPK3 Cell Signaling #95702, pRIPK3 Abcam #209384, RIP1 Cell Signaling #3493s, pRIP1 Cell Signaling #31122, MLKL Millipore Sigma #MABC604, and pMLKL Abcam #196436m.

NEONATAL RAT VENTRICULAR MYOCYTES. Female Sprague-Dawley rats and newborn litters were obtained from Charles River. Neonatal rat ventricular myocytes (NRVMs) were isolated as previously described.[27] Experiments were performed after 36 to 72 hours of serum starvation in the presence of insulin, transferrin, and bromodeoxyuridine.

LACTATE DEHYDROGENASE ASSAY. The supernatant from cultured NRVMs was collected to determine the content of lactate dehydrogenase (LDH) via cytotoxicity detection kit (Roche) following the manufacturer's instructions.

MITOCHONDRIAL MEMBRANE POTENTIAL ASSAY. Mitochondrial membrane potential (ΔΨm) in NRVMs was measured by 5, 5′, 6, 6′-tetrachloro-1, 1′, 3, 3′-tetraethylbenzimidazolylcarbocyanine iodide (JC-1) reduction. Cells were stained with JC-1 (Abcam) according to the manufacturer's protocol. In brief, after appropriate treatment, serum-starved NRVMs were exposed to JC-1 at 2 μM for 30 minutes. Cells were washed once with medium then analyzed by plate reader (CLARIO star, BMG LABTECH). JC-1 green fluorescence was excited at 488 nm and emission was detected using a 530 ± 40-nm filter. JC-1 red fluorescence was excited at 488 nm and emission was detected using a 613 ± 20-nm filter. A shift in fluorescence from red (JC-1 aggregates) to green (JC-1 monomers) indicates JC-1 dissociation from mitochondria into the cytosol, implying a reduction of ΔΨm.

RETROSPECTIVE COHORT CLINICAL STUDY. We conducted a retrospective observational study using clinical data from the Carolina Data Warehouse for Health. The study population consisted of all patients who were admitted to the UNC Healthcare system with a primary diagnosis of acute myocardial infarction (International Classification of Diseases [ICD]-9 code: 410 or ICD-10 code I21) and underwent PCI between January 2014 and December 2018. Patients were grouped according to whether they were discharged from the hospital with a prescription for an α-blocker. The prespecified primary outcome was defined as all-cause mortality before the end of the follow-up period (February 1, 2020).

STATISTICS. Baseline and clinical characteristics are presented for the clinical study population as the mean $\pm$ SD for continuous variables or count (percentage) for categorical variables. A Kaplan-Meier analysis was used to compare the unadjusted risk of death between groups using the log-rank test. A multivariable Cox proportional hazards model was used to estimate the adjusted HR and 95% CI. Models were adjusted for demographic or clinical values that

were significantly different between groups at baseline (age, sex, history of heart failure, history of hypertension). All analyses on clinical data were performed using R Statistical Software (R 3.3.0+, RStudio 2023.06.0+421).

STATISTICS (MOUSE STUDIES). The values of each parameter within a group are expressed as the mean ± SEM. Comparisons were performed using analysis of variance followed by Tukey post hoc tests (3 or more groups) or by Student t tests (2 groups) using GraphPad Prism 9. A $P < 0.05$ was considered statistically significant.

STUDY APPROVAL. Animal care and experimental protocols were approved by the University of North Carolina at Chapel Hill Institutional Animal Care and Use Committee and complied with Guide for the Care and the use of Laboratory Animals (National Research Council Committee for the Update of the Guide for the Care and Use of Laboratory Animals, 2011). The retrospective cohort clinical study was approved by the UNC Institutional Review Board (Institutional Review Board 19-3324). Written informed consent was obtained from all subjects before data collection.

RESULTS

GENERATION OF MICE WITH SPECIFIC DELETION OF THE α1A-AR IN CARDIOMYOCYTES.

To examine the functions of cardiomyocyte α1A-ARs, we created the cmAKO mouse line. We initially bred mice with Cre recombinase under the control of a truncated *Myh6* promoter with mice carrying the ROSA[mT/mG] Cre-reporter allele.[20] This approach allowed us to confirm Cre expression (green fluorescent protein [GFP+]) within the ventricle of *Myh6*-Cre/ROSA[mT/mG] mice but the absence of Cre expression (red fluorescent protein [RFP+]) in noncardiac tissues such as brain, kidney, and spleen (Figure 1A). We used a mouse line with low levels of Cre expression shown to be nontoxic (generated by E. Dale Abel and generously shared by Leslie Leinwand) rather than the more commonly used Myh6-Cre mice with higher and potentially deleterious levels of Cre expression.[21,28] To generate the cmAKO mice, we bred the *Myh6*-Cre mice with a mouse line harboring loxP sites flanking the first coding exon in *Adra1a* (the gene encoding the α1A-AR). To confirm cardiac-specific deletion of the α1A-AR in our cmAKO mice, we isolated RNA from heart as well as brain, kidney, and spleen. Using qRT-PCR, we determined that cmAKO mice exhibited a >90% reduction in α1A-AR mRNA in the heart, but preserved α1A-AR expression in all other tissues examined (Figure 1B). Expression of the α1B-AR (*Adra1b*) in the LV was unaffected by the Cre-lox

recombination event (Figure 1C). We then assayed for α1A-AR protein levels in isolated AMVMs from WT and cmAKO mice using competition radioligand binding with the α1A-selective antagonist 5-methylurapidil, as there are no reliable α1A-AR antibodies.[29] The binding curve for WT (Cre[negative]) AMVMs fit to a 2-site model, consistent with the presence of α1A (high affinity) and α1B-ARs (low affinity), whereas cmAKO AMVMs fit to a 1-site model, consistent with the presence of only the α1B-AR subtype (Figure 1D).

ABSENCE OF CARDIOMYOCYTE α1A-ARs DOES NOT ALTER BASELINE CARDIAC MASS OR FUNCTION.

Next, we examined the baseline cardiac function of our cmAKO mice and their littermates. As shown in Table 1, the absence of cardiomyocyte α1A did not affect either body weight or heart weight. Heart weight indexed to tibia length was identical in cmAKO mice and their littermates (Figure 1E), consistent with published phenotypes for global α1A-KO and α1A transgenic mice. Using conscious echocardiography to further characterize the cardiac structure and function of the cmAKO mice, we found that fractional shortening was 52% ± 8% in WT and 52% ± 9% in cmAKO mice (Table 1, Figure 1F). Collectively, these findings strongly suggest that the physiological cardiac hypertrophy induced by nonselective α1-AR agonists is mediated by the α1B subtype.[9] They also indicate that, although enhancing α1A activity preserves contractile function in the setting of injury, its presence is not required to maintain normal basal contractile function.[8]

CARDIOMYOCYTE α1A-ARs PROTECT AGAINST EARLY INJURY IN A PERMANENT LCA LIGATION MODEL.

After verification and basal characterization of our cmAKO and WT mice, we sought to test whether the absence of cardiomyocyte α1A-ARs affected the response to injury in an experimental model of MI. Towards this end, male cmAKO mice and their littermates were subjected to a well-established LCA ligation model. Of 15 WT and 17 cmAKO mice that underwent surgery, only 2 WT mice died between postoperative day 3 and day 10; however, 11 cmAKO mice died during this period. At 14 days post-infarction, survival in WT mice was 86.7% whereas survival in cmAKO mice was 35.3% ($P = 0.002$ by log-rank method) (Figure 2A). Given the striking difference in mortality, a subgroup of dead mice was subjected to necropsy with histological examination. We found evidence of LV rupture in 6 of 9 cmAKO mice, which was confirmed using published validated criteria showing coagulated blood in the chest cavity with disruption of the ventricle on gross examination

FIGURE 1   Validation of Mice Lacking Cardiomyocyte α1A-ARs
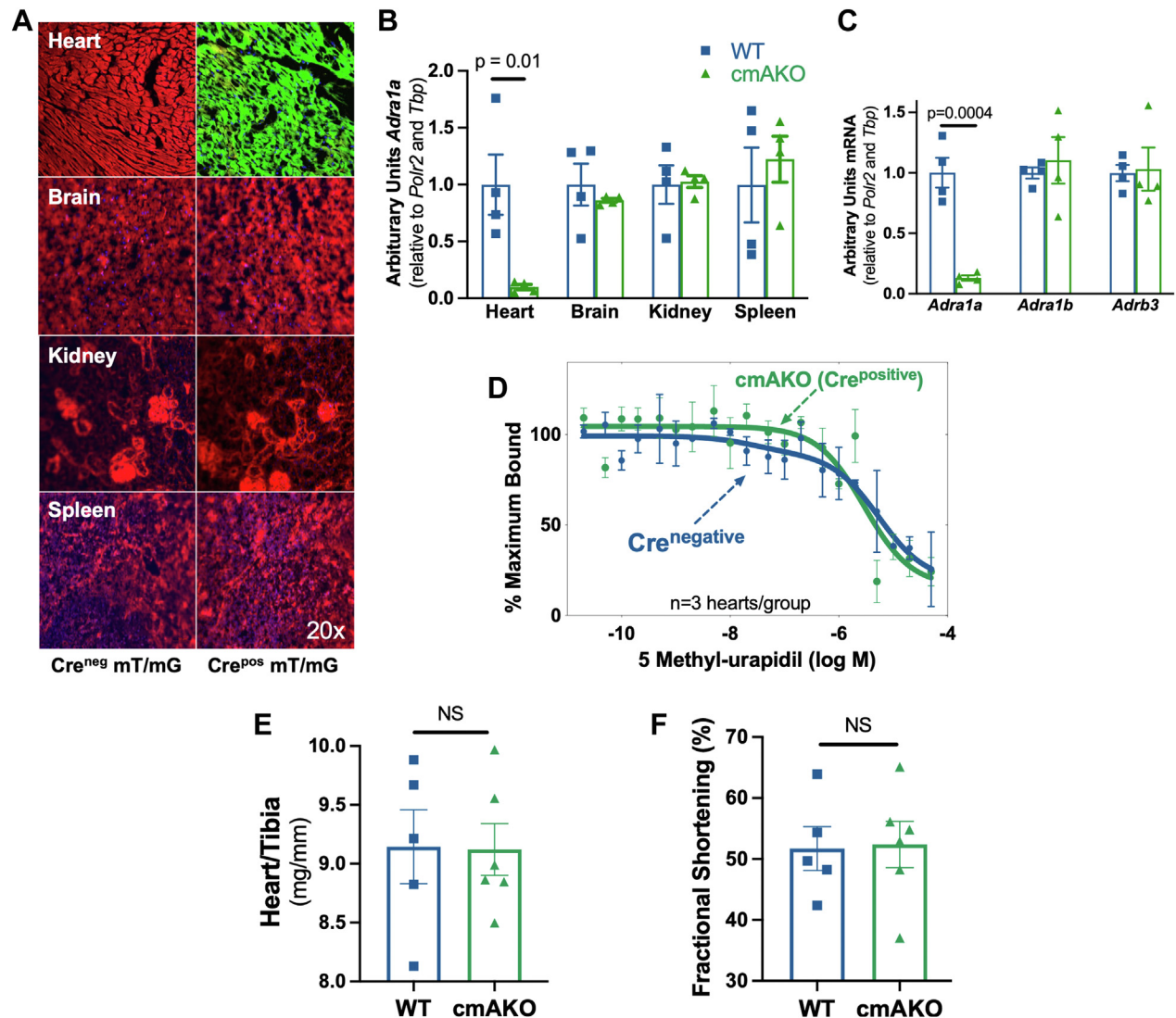
Mice were sacrificed at 12 to 16 weeks of age. (A) Representative images of heart, brain, and kidney in *Myh6*-Cre/ROSA^mT/mG mice. Green fluorescence indicates the presence of *Myh6*-Cre expression (Cre^pos) whereas red fluorescence indicates the absence of *Myh6*-cre expression (Cre^neg). (B) mRNA expression for the α1A-AR (*Adra1a*) on tissues from wild-type (WT; *Myh6*-Cre^neg/α1A-AR^fl/fl) and cardiomyocyte-specific alpha 1A knockout (cmAKO) littermates. (C) mRNA expression of α1A-AR and α1B-AR (*Adra1b*) in left ventricles of WT and cmAKO mice. (D) Competition radioligand binding in isolated adult mouse ventricular myocytes (n = 3 hearts per group) using the α1A antagonist 5 methyl-urapidil. (E) Heart weight indexed to tibia length. (F) Fractional shortening, as measured by conscious echocardiography. All comparisons used unpaired Student *t* tests. α1A-AR = alpha 1A adrenergic receptor; *Actb* = beta-actin; NS = not significant; *Tbp* = TATA binding protein.

(Supplemental Figure 1A).[30] Hematoxylin and eosin staining identified extensive coagulative necrosis and peri-infarct hemorrhage, providing histopathological context and pathobiological basis for ventricular rupture (Supplemental Figure 1B). Considering the excessive mortality by day 5, we turned our attention thereafter to an earlier timepoint, conducting all subsequent analyses at day 3 post-ligation. Using

established protocols for measuring infarct area, we found that cmAKO mice sustained 50% larger infarcts than WT mice (22% ± 2% LV mass vs 34% ± 3% LV mass, *P* = 0.015) by post-MI day 3 (Figure 2B).[25]

Changes in ventricular muscle tensile strength precede the onset of ventricular rupture in experimental acute MI.[31] We used a Biotester-5000 biaxial mechanical test system to determine

TABLE 1 Basal Cardiac Parameters in WT and cmAKO Mice (n = 6 Per Group)

	WT	cmAKO
HW, mg	153 ± 13	157 ± 9
BW, g	25.8 ± 2.1	25.9 ± 1.7
TL, mm	16.7 ± 0.7	17.2 ± 0.6
HW/BW, mg/g	5.9 ± 0.8	6.1 ± 0.4
HW/TL, mg/mm	9.1 ± 0.7	9.1 ± 0.5
Heart rate, beats/min	694 ± 37	634 ± 77
LV mass, mg	113 ± 5	103 ± 18
EF, %	83.4 ± 6.7	83.9 ± 8.5
FS, %	51.7 ± 8.0	52.4 ± 9.3

Values are mean ± SEM. An unpaired Student t test compared the 2 groups in each instance. No statistical differences between the 2 groups were found for any variables.

BW = body weight; cmAKO = cardiomyocyte-specific alpha 1A knockout; EF = ejection fraction by echocardiogram; FS = fraction shortening by echocardiogram; HW = heart weight; LV = left ventricle; TL = tibia length; WT = wild type.

whether mechanical properties differed in WT and cmAKO ventricles 3 days after MI, before the onset of cardiac rupture. To validate this system, we initially compared infarcted myocardium with myocardium from sham-operated animals and found that infarcted tissue showed an exponential stress-strain curve, consistent with previous reports.[32] We then compared the mechanical properties of sham-operated and infarcted WT and cmAKO mouse ventricles and found that the estimated biaxial tensile stretch (as in Ma et al)[33] was >70% higher in cmAKO mice (190 ± 34 vs 111 ± 42 kPa/% strain changes, $P = 0.004$) (**Figure 2C**, Supplemental Figure 2). These data suggested that the absence of cardiomyocyte α1A-ARs compromises the biomechanical adaption of the LV to experimental MI, potentially rendering the ventricle more susceptible to cardiac rupture.[34]

We then sought to determine whether this significant mechanical alteration at day 3 post-infarction was accompanied by other physiological indicators of injury. To determine whether infarct size correlated with circulating markers of cardiomyocyte death, we assayed serum HMGB1. HMGB1 is released by cells undergoing necrotic cell death and is recognized as a sensitive biomarker that correlates to the extent of cardiomyocyte death in patients with MI.[35] On day 3 after LCA ligation, serum HMGB1 from cmAKO mice was 58% higher than in WT controls (387 ± 56 pg/mL vs 244 ± 25 pg/mL, $P = 0.028$) (**Figure 2D**). Using a small-animal 9-T magnet for cardiac MRI, we then compared cardiac morphology and contractile function of WT and cmAKO mice 3 days after LCA ligation. Contractile function in cmAKO mice was significantly worse than in WT after infarction (26% ± 3% vs 34% ± 3%, $P = 0.037$) (**Figure 2E**) with evidence

of marked dyskinesis of the infarcted area (Video 1). LV mass indexed to body weight was 18% ± 3% lower in cmAKO than WT mice, consistent with greater cell death (**Figure 2E**).

Collectively these findings show that the absence of cardiomyocyte α1A-ARs is associated with a pronounced susceptibility to myocardial injury and death after experimental MI.

DEFICIENCY OF CARDIOMYOCYTE α1A-ARs RESULTS IN ACTIVATION OF RIP KINASES AND EXAGGERATED CELL DEATH. Our histopathological (**Figure 2B**) and serum biomarker (**Figure 2D**) data indicated that infarct-associated necrotic cell death was exacerbated by the absence of the cardiomyocyte α1A-AR. Although cellular necrosis historically has been regarded as a passive process, emerging evidence has shown clearly that programmed necrosis, or necroptosis, plays a critical role in numerous disease states including MI.[36,37] Necroptosis is initiated by binding of a ligand, often but not always a member of the tumor necrosis factor-α superfamily, to a cardiomyocyte death receptor. Death receptor activation promotes the assembly of the necrosome that includes the RIP kinases RIP1 and RIP3 and the terminal effector mixed lineage kinase domain-like protein (MLKL) leading to translocation of MLKL to the plasma membrane and necrosis. This signaling machinery is distinct from apoptotic signaling and activation typically requires intrinsic inhibition of apoptosis (reviewed in Del Re et al[36]).

To probe the contributions of necroptosis and apoptosis to the dramatic cmAKO phenotype and to define whether cardiomyocyte α1A-ARs differentially constrained necroptosis and apoptosis in the setting of MI, we immunoblotted for canonical mediators of each process in WT and cmAKO mice 3 days after LCA ligation. RIP1 and RIP3 expression were 2-fold higher in the border zone of infarcted cmAKO hearts compared to infarcted WT controls (**Figure 3A**), consistent with activation of the necrosome. In contrast, the expression level of cleaved caspase-3 (c-Casp-3) and cleaved PARP was no different between the 2 groups (**Figure 3A**, Supplemental Figure 3). We then asked whether the terminal necroptosis effector MLKL was differentially upregulated in the infarct border zone of cmAKO mouse hearts. Immunofluorescent staining revealed that MLKL was almost entirely absent in the myocardium of sham-operated control animals (**Figure 3B**). In contrast, the border zone of infarcted animals contained markedly higher expression of MLKL within cardiomyocytes, as defined using wheat germ agglutinin. Qualitative evaluation suggested that cmAKO hearts contained

FIGURE 2 Disruption of the Cardiomyocyte α1A-AR Decreases Survival and Exacerbates Cardiac Dysfunction After Experimental Myocardial Infarction
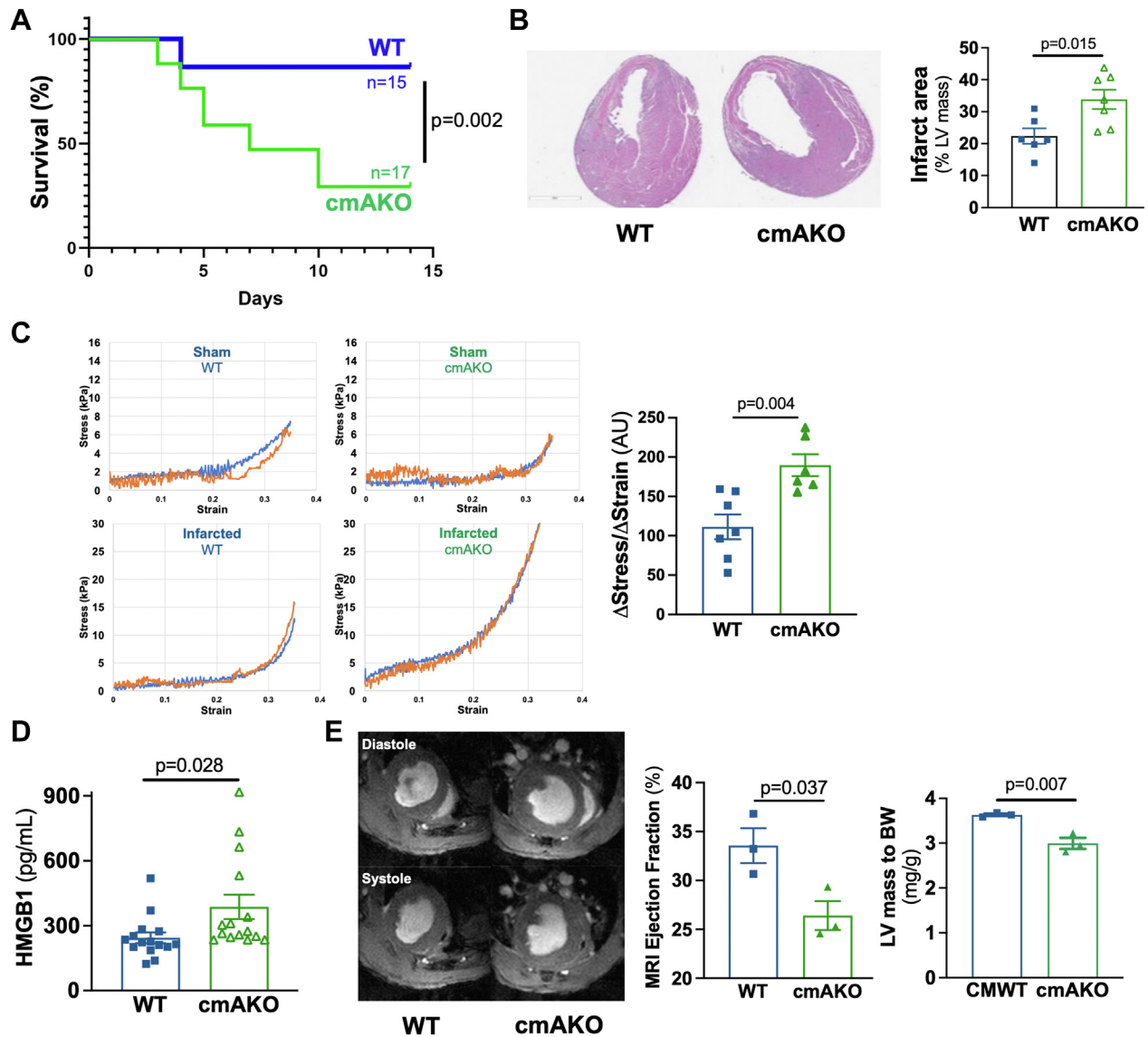
Male WT and cmAKO mice underwent permanent ligation of the left coronary artery to create a myocardial infarction. (A) Kaplan-Meier survival plot (log-rank test). (B) Infarct area calculated from summed slices in Image J. (C) Left ventricular (LV) mechanical properties as measured by a Biotester-5,000 biaxial mechanical test apparatus. (D) Enzyme-linked immunosorbent assay compared serum abundance of high mobility group box 1 (HMGB1) in WT and cmAKO mice after infarction. (E) Cardiac magnetic resonance imaging (MRI) quantified LV contractile function and structure, as indicated by ejection fraction and LV mass indexed to body weight (BW). Comparisons in B through E used unpaired Student t tests.

more MLKL than WT (Myh6-Cre[neg]/Adra1a^{fl/fl}). Nuclear staining with DAPI identified robust infiltration of leukocytes consistent with the immune response that is activated by necrotic loss of cardiomyocyte membrane integrity. We then immunoblotted for MLKL to quantify its abundance in the border zone. We found that MLKL, relative to total protein, increased almost 8-fold in cmAKO animals but was not significantly changed in WT animals (**Figure 3C**).

Taken together, these results suggest that RIP1/3 mediated cardiomyocyte necroptosis, but not apoptosis, was exaggerated in mice lacking cardiomyocyte α1A-ARs after experimental MI.

A SELECTIVE α1A-AR AGONIST PROTECTS AGAINST RIP KINASE–MEDIATED CARDIOMYOCYTE DEATH IN VITRO. To expand upon our in vivo findings showing that the absence of cardiomyocyte α1A-ARs was associated with enhanced cell death and RIP kinase

FIGURE 3 Mediators of Necroptosis, But Not Apoptosis, Are Upregulated to a Greater Extent in cmAKO Than WT Mice After Myocardial Infarction
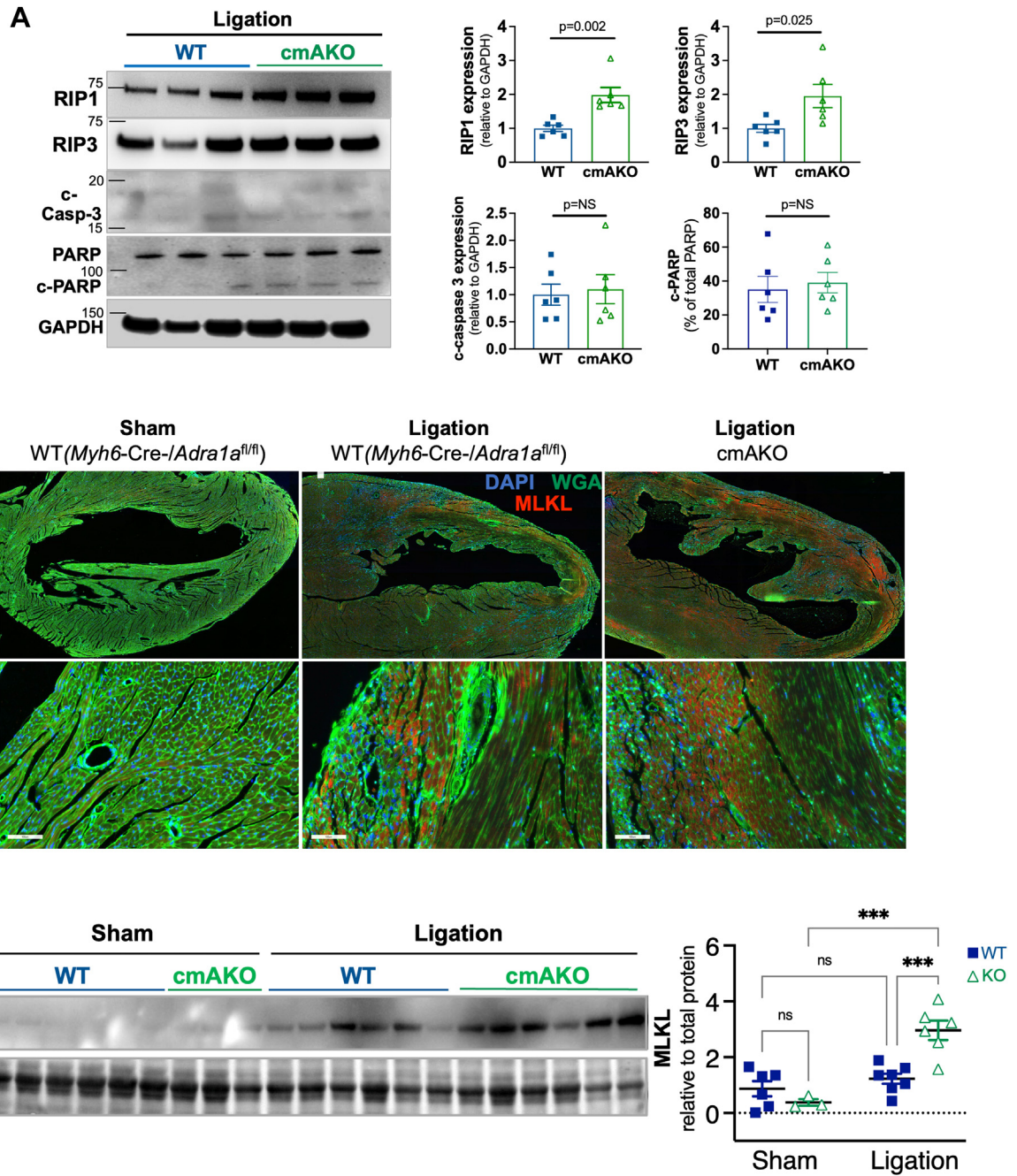
Tissue was excised from the border zone of the LV infarct 3 days after left coronary artery ligation. (A) Immunoblotting for mediators of necroptosis (receptor interactor proteins [RIPs] 1 and 3) and apoptosis (c-PARP and cleaved caspase 3 [c-Casp3]) with representative image and summary densitometry. (B) Immunofluorescence for the necroptosis effector mixed lineage kinase domain–like (MLKL) protein. (C) Immunoblotting for MLKL with representative images and summary densitometry summary densitometry (relative to total membrane protein, Supplemental Figure 4B). Comparisons between 2 groups (A and B) used unpaired Student *t* tests. Comparisons between 4 groups (C) used a 2-way analysis of variance with a Tukey post-test. KO = knockout; PARP = poly ADP-ribose polymerase; GAPDH = glyceraldehyde-3-phosphate dehydrogenase; other abbreviations as in **Figures 1 and 2**.

upregulation, we used a well-established in vitro model of ischemia induced by exposing primary NRVMs to oxygen and glucose deprivation (OGD).[38] As indicated in **Figure 4A**, 24 hours of OGD resulted in significant cell injury as determined by LDH release when compared to standard culture conditions (34% ± 5% vs 3% ± 1% of positive control, $P < 0.0001$). Cell death was mitigated by selective α1A activation (A61603, 100 nM) or by nonselective α1-AR activation with the combination of NE (100 nM) and the β-AR antagonist (β-blocker) propranolol (1 μM). Next, we examined whether α1A-AR activation would protect against mitochondrial injury, as RIP3 activation promotes mitochondrial permeability transition pore opening and resultant loss of $\Delta\Psi m$.[39] Using the mitochondrial membrane permeant dye JC-1 (red aggregate with intact $\Delta\Psi m$, green monomer with compromised $\Delta\Psi m$) we found that 6 hours of OGD exposure led to a profound loss of $\Delta\Psi m$ that was partially rescued by coadministration of A61603 (205% ± 44% vs 107% ± 37% aggregate/monomer, $P = 0.005$) (**Figure 4B**).

To define further the importance of RIP kinases and necroptosis in our model systems, we used necrostatin-1stable (Nec-1s), a highly selective inhibitor of RIPK1.[40] RIPK1 inhibitors, including Nec-1s have been shown to limit necrotic cell death due to ischemia in the heart and other organs and have been proposed as novel therapies for multiple disease processes mediated by ischemia.[41-43] Here we exposed NRVMs to OGD in the presence or absence of the α1A agonist A61603 (A6) or Nec-1s 50 μM (**Figures 4C to 4E**). A61603 and Nec-1s both decreased OGD-induced RIP1 by 50% and combination treatment further blunted RIP1 expression. Both A61603 and Nec-1s decreased RIP3 expression by 60% to 70%, but no additive effect was observed. Neither α1A activation nor RIP1 inhibition affected expression of the apoptosis mediators c-Casp-3 or cleaved PARP (**Figure 4C**). A61603 and Nec-1s both independently mitigated NRVM death (**Figure 4D**) and protected NRVM $\Delta\Psi m$ (**Figure 4E**), but no additive effect of α1A activation and RIPK1 inhibition was observed for these endpoints. A61603 did not affect expression of RIP1 or RIP3 in normoxic NRVMs (Supplemental Figure 4C).

Collectively, these findings show that pharmacologic activation of α1A-AR protects against ischemia-induced RIP kinase activation and necroptotic cell death. The absence of synergistic benefit from concomitant α1A activation and RIP inhibition raises the possibility that abrogation of necroptosis may contribute significantly to α1A-mediated cytoprotection. These in vitro results using NRVMs exposed to OGD are consistent with the findings from our LCA ligation model, suggesting that in vivo RIP kinase pathway activation likely results from cardiomyocyte necroptosis that is enhanced in the absence of the α1A-AR.

TREATMENT WITH THE RIP1 KINASE INHIBITOR NEC-1S MITIGATES INJURY IN cmAKO MICE AFTER LCA LIGATION.
Our in vitro studies using NRVMs suggested that mitigation of necroptosis contributes to the cytoprotective effects of an α1A-AR agonist in the setting of ischemia. As an extension of these findings, we then sought to test whether inhibition of necroptosis in vivo could blunt the exaggerated response to injury in cmAKO mice using our experimental MI model.

To address this question, WT and cmAKO mice were administered Nec-1s (1.65 mg/kg body weight) or vehicle intravenously 10 minutes before LCA ligation, followed by daily intravenous injection for 2 days before sacrifice on day 3. Infarct size on day 3 was no different in the cmAKO (20% ± 2% LV surface area) than the WT mice (16% ± 2%), a contrast to the significant difference between genotypes in the absence of Nec-1s (WT 34% ± 8% vs cmAKO 22% ± 6%, $P = 0.015$) (**Figure 2B, Figure 5A**, Supplemental Figure 5). Serum levels of the necrotic cell death marker HMGB1 were markedly higher in cmAKO than WT mice after infarct, but Nec-1s treatment abrogated that difference (**Figure 5B**). These findings suggested that necroptotic cell death accounted for the difference in HMGB1 release in WT and cmAKO mice and that HMGB1 may be a reliable biomarker for necroptosis post-MI. Consistent with findings from our previous experiments (**Figure 4A**), RIP1 (1.6-fold) and RIP3 (2-fold) were activated to a greater extent in the infarct border zones of cmAKO than WT mice (**Figure 5C**). Nec-1s treatment blunted RIP1 and RIP3 in all mice and abrogated the difference between the genotypes (**Figure 5C**).

Taken together, these findings suggest that RIP1 kinase–mediated necroptosis contributes significantly to enhanced susceptibility to ischemic injury in the absence of cardiomyocyte α1A-ARs.

ALPHA BLOCKER EXPOSURE INCREASES MORTALITY AFTER MI IN MEN.
Next, we sought to determine whether the loss of α1-AR function also confers worse post-infarct outcomes in humans. Antagonists of α1-ARs (α-blockers) were developed to treat hypertension but currently are used most frequently to treat lower urinary tract symptoms due to benign prostatic hyperplasia in older men. Previous studies have

FIGURE 4 Pharmacologic Activation of α1A-ARs Protects Neonatal Rat Ventricular Myocytes From Experimental Ischemia
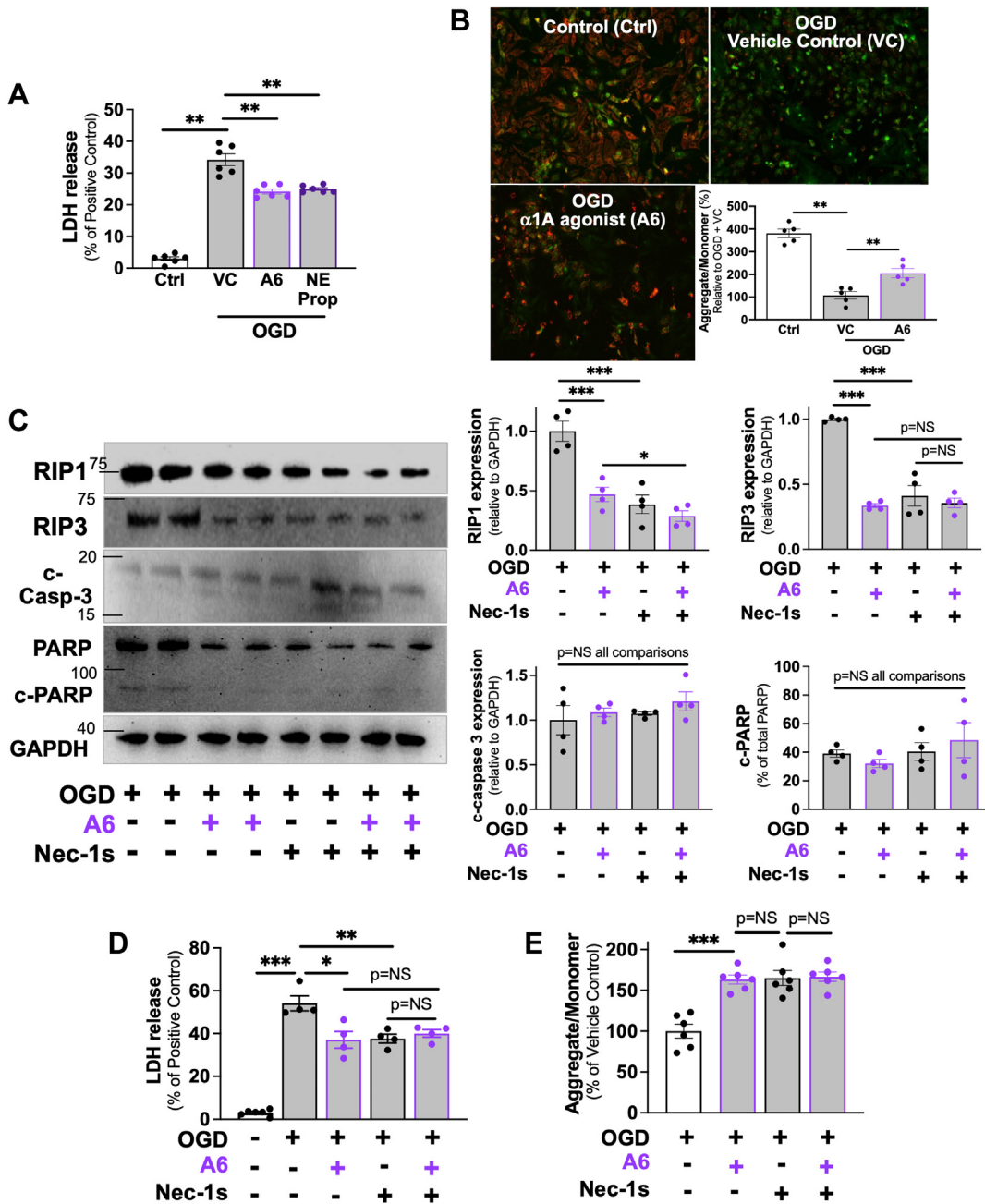
Ischemia was simulated in neonatal rat ventricular myocytes (NRVMs) using oxygen glucose deprivation (OGD) for 24 hours in vehicle cont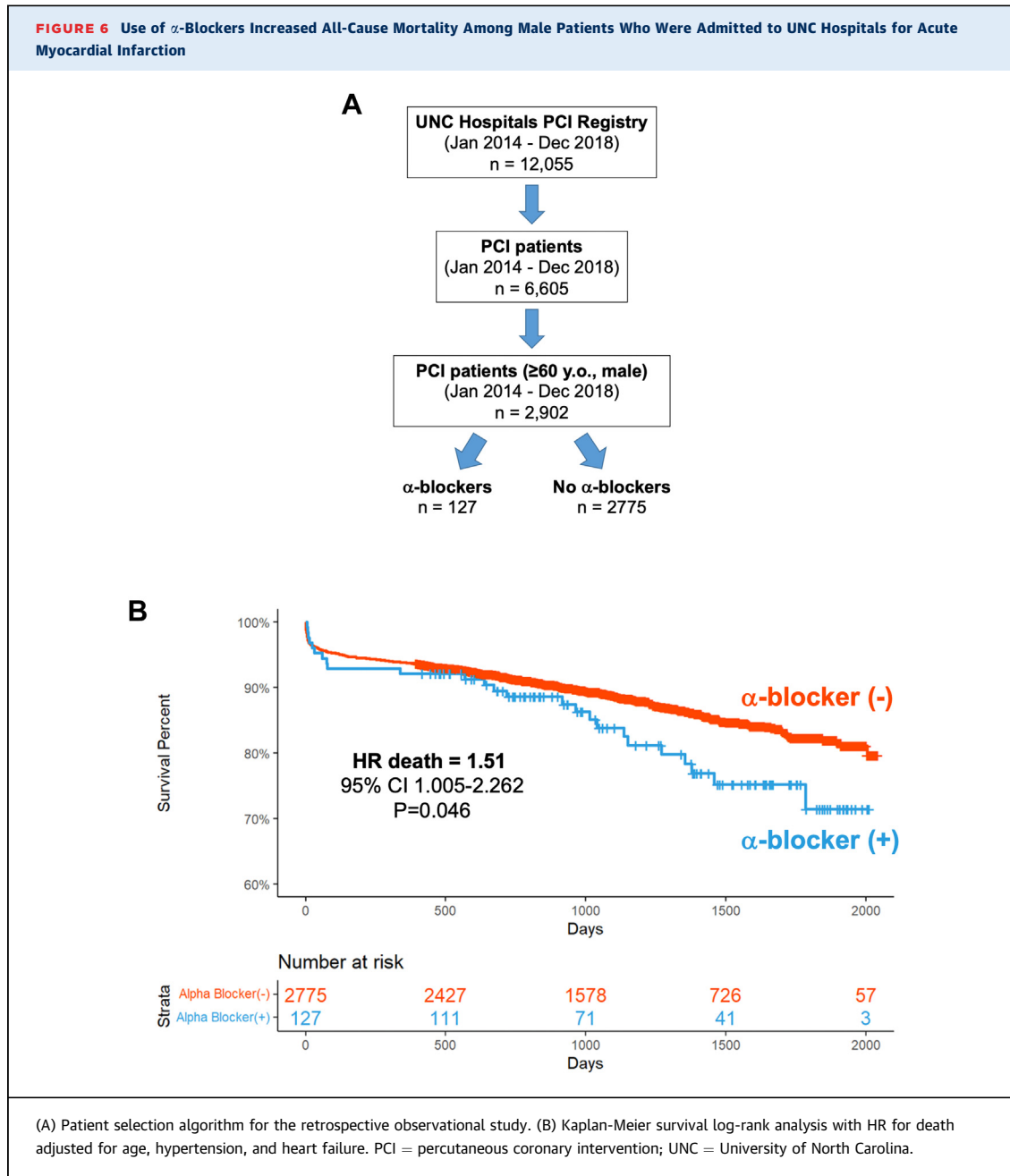rol (VC) with or without the α1A-AR agonist A61603 100 nM or the nonselective AR agonist norepinephrine (NE, 1 mM) with the β-AR antagonist propranolol (Prop, 1 mM), or the RIP1 kinase antagonist Nec-1s 50 mM. (A) Lactate dehydrogenase (LDH) measured cell death relative to positive control. (B) The mitochondrial membrane permeant dye JC-1 measured mitochondrial membrane potential (ΔΨm) where red indicates intact ΔΨm and green indicates compromised ΔΨm. (C) Cell lysates from OGD-exposed NRVMs in the presence or absence of A61603 or Nec-1s for 6h were immunoblotted. Image J measured relative densitometry. (D) LDH release measured OGD-exposed NRVM death after 6 hours in the presence or absence of A61603 or Nec-1s. (E) JC-1 measured NRVM ΔΨm in the presence or absence of A61603 or Nec-1s for 6 hours. *$P < 0.05$. **$P < 0.01$. ***$P < 0.001$ by analysis of variance with Tukey post-test. N > 3 technical replicates per experiment. Abbreviations as in **Figures 1 and 3**.

FIGURE 5 Treatment With the RIP1 Kinase Inhibitor Nec-1s Mitigates the Exaggerated Response to Injury in cmAKO Mice Subjected to Left Coronary Artery Ligation

Male WT and cmAKO mice were injected intravenously with Nec-1s (1.65 mg/kg body weight) or vehicle 10 minutes before left coronary artery ligation, followed by daily intravenous injection for 2 days before sacrifice on day 3. (A) Infarct area was calculated histologically. (B) Serum level of HMGB1, a measure of necrotic cell death was measured using an enzyme-linked immunosorbent assay. (C) Lysates were prepared from the infarct border zones of all mice and immunoblotted for mediators of necroptosis (RIP1 and RIP3 kinases) and apoptosis (c-Casp-3 and c-PARP). Summary densitometry was calculated in Image J. $*P < 0.05$. $**P < 0.01$. $***P < 0.001$ by analysis of variance (ANOVA) with Tukey post-test. Comparisons between 2 groups (A) used unpaired Student t tests. Comparisons between 4 groups (B and C) used a 2-way ANOVA with a Tukey post-test. Abbreviations as in **Figures 1 to 4**.

identified an association between α-blocker use and incident HF, but the effect of α-blockers on outcomes after MI has never been studied.[44,45] We conducted a retrospective observational study using clinical data from the UNC Hospitals PCI Registry within the Carolina Data Warehouse for Health. We initially identified all patients (n = 12,055) who were admitted to the UNC Healthcare system with a primary diagnosis of acute MI (ICD-9: 410 or ICD-10: I21) and underwent PCI between January 2014 and December 2018

(**Figure 6A**). From this population, we merged instances with identical medical record numbers (the same patient admitted to the hospital multiple times) and filtered out patients younger than 60 years and women, as α-blockers rarely are prescribed to either group. The prespecified primary outcome was defined as all-cause mortality before the end of the follow-up period (February 1, 2020).

This selection algorithm identified 127 male patients taking α-blockers and 2,775 male patients not

FIGURE 6 Use of α-Blockers Increased All-Cause Mortality Among Male Patients Who Were Admitted to UNC Hospitals for Acute Myocardial Infarction

(A) Patient selection algorithm for the retrospective observational study. (B) Kaplan-Meier survival log-rank analysis with HR for death adjusted for age, hypertension, and heart failure. PCI = percutaneous coronary intervention; UNC = University of North Carolina.

taking α-blockers at the time of their MI. The α-blocker (+) patients were older than the α-blocker (−) patients, but otherwise were clinically and demographically similar (**Table 2**). Our analysis found that the crude all-cause mortality rate at 3 years post-MI follow-up was higher in α-blocker (+) patients (19.7% vs 12.5%, $P = 0.019$). Applying a Cox proportional hazards regression model with adjustment for age, history of hypertension and history of HF, we found that the HR for death in the α-blocker (+) post-MI

male patients was 1.51 (95% CI: 1.01-2.26; $P = 0.046$) (**Figure 6B**). A Schoenfeld individual test was performed and confirmed that our dataset fits the proportional hazard assumption.

DISCUSSION

In this study we show that mice with cardiomyocyte-restricted deletion of the α1A-AR exhibit a significantly elevated risk of death within the first 5 days

TABLE 2 Clinical and Demographic Characteristics of Male Patients ≥60 years of Age Who Underwent Percutaneous Coronary Intervention (PCI) After Admission to UNC Hospital for Acute Myocardial Infarction

	α-Blocker Use			
	Yes (n = 127)	No (n = 2,775)	Overall (n = 2,902)	P Value
Male	127 (100)	2,775 (100)	2,902 (100)	
Age at PCI, y	73.0 ± 7.87	70.7 ± 7.11	70.8 ± 7.16	0.002
Race				0.39
AA	11 (8.7)	313 (11.3)	324 (11.2)	
White	108 (85.0)	2,330 (84.0)	2,438 (84.0)	
Other	8 (6.3)	132 (4.8)	140 (4.8)	
Smoking	25 (19.7)	623 (22.5)	648 (22.3)	0.46
Chronic lung disease	19 (15.0)	378 (13.6)	397 (13.7)	0.67
Cerebrovascular disease	26 (20.5)	468 (16.9)	494 (17.0)	0.30
Diabetes	55 (43.3)	1,167 (42.1)	1222 (42.1)	0.80
HTN	115 (90.6)	2,416 (87.1)	2,531 (87.2)	0.27
HLD	104 (81.9)	2,342 (84.4)	2,446 (84.3)	0.39
LVEF, %				0.10
0-50	24 (18.9)	556 (20.0)	580 (20.0)	
50+	57 (44.9)	1,452 (52.3)	1,509 (52.0)	
GFR, mL/min				0.33
<60	46 (36.2)	832 (30.0)	878 (30.3)	
>60	76 (59.8)	1,828 (65.9)	1,904 (65.6)	

Values are n (%) or mean ± SD. An unpaired Student t test compared the 2 groups in each instance.

AA = African American; PCI = percutaneous coronary intervention; GFR = glomerular filtration rate; HTN = hypertension; HLD = hyperlipidemia; LVEF = left ventricular ejection fraction.

after experimental MI. These new cmAKO mice developed larger infarcts with exaggerated ventricular remodeling and contractile dysfunction within 3 days post-infarct compared to WT controls. In vitro studies corroborated these findings, showing that α1A-AR activation limits cell death in the setting of ischemic injury. These striking findings prompted us to perform in vivo and in vitro studies which collectively suggested that constraint of necroptosis contributes to cardioprotection by cardiomyocyte α1A-ARs. A retrospective observational clinical study at our institution indicated that the use of medications that block α1-ARs was associated with increased risk of mortality after MI in men, offering a potential clinical parallel for our experimental findings.

To the best of our knowledge, our study is the first to show an essential protective role for endogenous cardiomyocyte α1A-ARs in response to injury using a cardiomyocyte-specific loss-of-function model. Mice with 66-fold overexpression of rat *Adra1a* have improved survival and contractile function 15 weeks after LCA ligation.[17] Transgenic overexpression (15- to 40-fold) of the α1A-AR in rat cardiomyocytes confers enhanced protection in the second window of

ischemic preconditioning and is associated with decreased ventricular remodeling and enhanced angiogenesis 4 to 6 weeks after MI.[18,46] Global α1A-AR KO mice have increased mortality and enhanced ventricular remodeling 4 weeks after MI.[19] Here we created a cardiomyocyte-specific α1A-AR KO mouse line to avoid the potentially confounding effects of either supraphysiological protein abundance in the heart or systemic effects from global deletion of a widely expressed receptor. Our cmAKO mice have normal basal cardiac structure and function (**Figure 1**, **Table 1**), similar to both the global α1A-KO mice and to a recently published line with inducible cardiomyocyte-specific α1A-AR deletion.[19,47] Although deletion of cardiomyocyte α1A-ARs does not alter basal phenotype appreciably, it does confer significantly enhanced susceptibility to injury, as evidenced by 50% mortality within 5 days of MI in this study.

Here we, by necessity, have focused our mechanistic analyses on an earlier time point given the excessive mortality within 5 days post-MI due primarily to cardiac rupture (66.7%, n = 6 of 9) as confirmed by standardized methodology.[30] Our

observations from biaxial tensile tests confirmed that disruption of cardiomyocyte α1A-ARs leads to maladaptive biomechanical properties in the infarct and peri-infarct zones predisposing to ventricular rupture. Although the propensity for post-MI cardiac rupture likely is multifactorial, extensive necrotic loss of cardiomyocytes primes the myocardium to rupture via proinflammatory responses and dynamic changes in the extracellular matrix.[48-50] Historically, necrosis has been considered an "unregulated" and passive form of cell death. However, studies performed over the past 2 decades have unequivocally characterized necroptosis as a regulated form of cellular necrosis that plays critical roles in multiple types of cardiac pathology, including myocardial ischemia and infarction.[36,39,51-53]

The early post-infarct period is characterized by elevated levels of endogenous catecholamines that activate ARs on cardiomyocytes.[54] High concentrations of the β-AR agonist isoproterenol (85 mg/kg subcutaneous) induce cardiomyocyte necrosis with induction of RIP1 and RIP3 in mice, suggesting that β-AR hyperactivation may promote necroptosis to contribute to the pathobiology of MI.[55] Regulation of necroptosis by α1-ARs has not been studied previously. Here, we report that endogenous α1A-ARs protect cardiomyocytes after MI in part by constraining RIP kinase–MLKL–mediated necroptosis, but not apoptosis. Our findings would appear to be inconsistent with a previously published study showing enhanced myocardial apoptosis after experimental MI in global α1A-AR KO mice.[19] However, there are several important differences in the design of these studies that may explain the apparent discrepancies. Yeh et al[19] analyzed the infarcted heart 4 weeks after LCA ligation, whereas here we performed most of our studies in mice 3 days after ligation. This temporal difference may be important given that the predominant modes of cell death vary with time after infarction.[56] In addition, Yeh et al[19] assayed cell death from remote non-infarcted myocardium, whereas we exclusively used tissues from the peri-infarct border zone. Lastly, it is entirely plausible that their findings were influenced by systemic loss of α1A-ARs, whereas we used a cardiomyocyte-specific KO mouse model. Although the global α1A-KO animals are a more faithful genetic representation of the potential systemic effects of α-blockers in humans, we created and used the cmAKO mice to focus specifically on events mediated directly by α1A-ARs in the heart.

Our study is also the first to report on enhanced risk of mortality in patients taking α-blockers, although other studies have identified an association between α-blockers and incident HF. In the landmark ALLHAT (Antihypertensive and Lipid Lowering treatment to prevent Heart Attack Trial), subjects receiving doxazosin had a 2-fold higher risk of developing HF than patients taking chlorthalidone.[44] Partly as a result of this finding, nonselective α-blockers no longer are considered first-line therapy for hypertension. However, α-blockers remain the most prescribed medication for managing symptomatic benign prostatic hyperplasia (BPH), which affects more than 70% of U.S. males 60 years of age or older.[57] In fact, the Medical Expenditure Panel Survey (Agency for Health Care Research and Quality) estimates that more than 5 million patients were prescribed the α1A-AR selective antagonist tamsulosin in the United States in 2019. A recent population-based study from Canada found that men receiving α-blockers for BPH had an increased risk of developing HF (HR: 1.22; 95% CI: 1.18-1.26) when compared to men with BPH who were not on medical therapy.[45] Neither of the previous studies reported increased mortality related to α-blockers as we do, although we studied a particularly high-risk population in post-MI patients.

STUDY LIMITATIONS. The complex pathobiology of MI is both spatially and temporally heterogeneous. We chose, by necessity, to focus our analyses on selected post-infarct time points and were painstaking in our efforts to study infarct border zone, but we cannot exclude the possibility that the α1A-AR regulates distinct processes at other times or in different myocardial locations after infarct. It is possible that alternative mechanisms other than necroptosis may contribute to the cardioprotective effects of cardiomyocyte α1A-ARs. For example, rats with cardiomyocyte-specific α1A-AR overexpression exhibited attenuated post-infarct remodeling characterized in part by enhanced formation of coronary collaterals mediated by vascular endothelial growth factor A.[18] We also cannot exclude the possibility that developmental effects contributed to the exaggerated susceptibility to injury in our cmAKO mice. In this regard, it would be interesting to study the response in a conditional knock down model such as the one recently created by Kaidonis et al[47], which also could allow for explication of the role of α1A-ARs in the more remote post-infarct period. Finally, our clinical study is relatively small and drawn from a single

medical center. It will be important to determine whether the increased risk of post-MI mortality can be replicated in larger datasets of patients receiving α-blockers.

CONCLUSIONS

Our study significantly advances our understanding of the mechanisms underlying the cardioprotective effects of the α1A-AR, identifying a previously unrecognized mechanistic connection with necroptosis. The marked susceptibility to injury of our novel cardiomyocyte-specific α1A-AR KO mouse suggests that enhanced cardiovascular risk in patients taking α-blockers may arise directly from inhibition of adaptive functions of cardiomyocyte α1A-ARs rather than systemic effects.

ADDRESS FOR CORRESPONDENCE: Dr Brian C. Jensen, Division of Cardiology, University of North Carolina,160 Dental Circle, CB 7075, Chapel Hill, North Carolina 27599-7075, USA. E-mail: bcjensen@med.unc.edu.

PERSPECTIVES

COMPETENCY IN MEDICAL KNOWLEDGE: Chronic stimulation of β-ARs contributes significantly to the pathobiology of HF through extensively explicated pathways. In contrast, an emerging literature indicates that α1A-ARs protect the heart by mitigating the toxic effects of chronic β-AR activation. The mechanisms underlying this cardioprotective benefit remain poorly defined. Defining these mechanisms more clearly could have significant clinical impact, as α1-AR antagonists (α-blockers) are associated with increased risk for developing HF.

TRANSLATIONAL OUTLOOK: Here we couple translational studies of MI in a new cardiomyocyte-specific α1A-AR KO mouse with a clinical study of patients taking α-blockers at the time of MI. We identify constraint of programmed cardiomyocyte necrosis (necroptosis) as a novel mechanism of α1A-AR cardioprotection in mice. We also find that patients taking an α-blocker at the time of MI experienced increased mortality during a follow-up period of over 5 years at our center, the first demonstration that α-blockers may affect survival in high-risk patients. These clinical findings suggest caution in the use of α-blockers in patients with ischemic heart disease and our preclinical studies indicate that this potential hazard arises from blocking adaptive signaling through α1A-ARs in cardiomyocytes. Future preclinical studies will explore other potential cardioprotective functions for α1A-ARs; future clinical studies will determine whether α-blockers confer increased risk after MI in larger multicenter datasets.

REFERENCES

1. Virani SS, Alonso A, Aparicio HJ, et al. Heart disease and stroke statistics – 2021 update: a report from the American Heart Association. *Circulation*. 2021;143:e254–e743.

2. Jenca D, Melenovsky V, Stehlik J, et al. Heart failure after myocardial infarction: incidence and predictors. *ESC Heart Fail*. 2021;8:222–237.

3. Konstantinidis K, Whelan RS, Kitsis RN. Mechanisms of cell death in heart disease. *Arterioscler Thromb Vasc Biol*. 2012;32:1552–1562.

4. Hogarth AJ, Mackintosh AF, Mary DA. The sympathetic drive after acute myocardial infarction in hypertensive patients. *Am J Hypertens*. 2006;19:1070–1076.

5. Jardine DL, Charles CJ, Ashton RK, et al. Increased cardiac sympathetic nerve activity following acute myocardial infarction in a sheep model. *J Physiol*. 2005;565:325–333.

6. Ziegler KA, Ahles A, Wille T, Kerler J, Ramanujam D, Engelhardt S. Local sympathetic denervation attenuates myocardial inflammation and improves cardiac function after myocardial infarction in mice. *Cardiovasc Res*. 2018;114:291–299.

7. O'Gara PT, Kushner FG, Ascheim DD, et al. 2013 ACCF/AHA guideline for the management of ST-elevation myocardial infarction: a report of the American College of Cardiology Foundation/ American Heart Association task force on practice guidelines. *J Am Coll Cardiol*. 2013;61:e78–e140.

8. Jensen BC, O'Connell TD, Simpson PC. Alpha-1-adrenergic receptors in heart failure: the adaptive arm of the cardiac response to chronic catecholamine stimulation. *J Cardiovasc Pharmacol*. 2014;63:291–301.

9. O'Connell TD, Jensen BC, Baker AJ, Simpson PC. Cardiac alpha1-adrenergic receptors: novel aspects of expression, signaling mechanisms, physiologic function, and clinical importance. *Pharmacol Rev*. 2014;66:308–333.

10. Jensen BC, Swigart PM, De Marco T, Hoopes C, Simpson PC. {alpha}1-Adrenergic receptor

subtypes in nonfailing and failing human myocardium. *Circ Heart Fail*. 2009;2:654–663.

11. O'Connell TD, Ishizaka S, Nakamura A, et al. The a1A/C- and a1B-adrenergic receptors are required for physiological cardiac hypertrophy in the double-knockout mouse. *J Clin Invest*. 2003;111:1783–1791.

12. Jensen B, Swigart P, Laden M-E, DeMarco T, Hoopes C, Simpson P. The alpha-1D is the predominant alpha-1-adrenergic receptor in human epicardial coronary arteries. *J Am Coll Cardiol*. 2009;54:1137–1145.

13. Chalothorn D, McCune DF, Edelmann SE, et al. Differential cardiovascular regulatory activities of the alpha 1B- and alpha 1D-adrenoceptor subtypes. *J Pharmacol Exp Ther*. 2003;305:1045–1053.

14. Cleveland JC Jr, Meldrum DR, Rowland RT, et al. Ischemic preconditioning of human myocardium: protein kinase C mediates a permissive role for alpha 1-adrenoceptors. *Am J Physiol*. 1997;273:H902–H908.

15. Banerjee A, Locke-Winter C, Rogers KB, et al. Preconditioning against myocardial dysfunction after ischemia and reperfusion by an alpha 1-adrenergic mechanism. *Circ Res*. 1993;73:656–670.

16. Zhang J, Simpson PC, Jensen BC. Cardiac alpha1A-adrenergic receptors: emerging protective roles in cardiovascular diseases. *Am J Physiol Heart Circ Physiol*. 2021;320:H725–H733.

17. Du XJ, Gao XM, Kiriazis H, et al. Transgenic alpha1A-adrenergic activation limits post-infarct ventricular remodeling and dysfunction and improves survival. *Cardiovasc Res*. 2006;71:735–743.

18. Zhao X, Balaji P, Pachon R, et al. Over-expression of cardiomyocyte alpha 1A-adrenergic receptors attenuates postinfarct remodeling by inducing angiogenesis through heterocellular signaling. *Arterioscler Thromb Vasc Biol*. 2015;35:2451–2459.

19. Yeh CC, Fan Y, Xu Y, Yang YL, Simpson PC, Mann MJ. Shift toward greater pathologic post-myocardial infarction remodeling with loss of the adaptive hypertrophic signaling of alpha1 adrenergic receptors in mice. *PLoS One*. 2017;12: e0188471.

20. Abel ED, Kaulbach HC, Tian R, et al. Cardiac hypertrophy with preserved contractile function after selective deletion of GLUT4 from the heart. *J Clin Invest*. 1999;104:1703–1714.

21. Pugach EK, Richmond PA, Azofeifa JG, Dowell RD, Leinwand LA. Prolonged Cre expression driven by the alpha-myosin heavy chain promoter can be cardiotoxic. *J Mol Cell Cardiol*. 2015;86:54–61.

22. O'Connell TD, Rodrigo MC, Simpson PC. Isolation and culture of adult mouse cardiac myocytes. *Methods Mol Biol*. 2007;357:271–296.

23. Myagmar BE, Flynn JM, Cowley PM, et al. Adrenergic receptors in individual ventricular myocytes: the beta-1 and alpha-1B are in all cells, the alpha-1A is in a subpopulation, and the beta-2

and beta-3 are mostly absent. *Circ Res*. 2017;120: 1103–1115.

24. Ruiz-Villalba A, Romero JP, Hernandez SC, et al. Single-cell RNA sequencing analysis reveals a crucial role for CTHRC1 (collagen triple helix repeat containing 1) cardiac fibroblasts after myocardial infarction. *Circulation*. 2020;142:1831–1847.

25. Takagawa J, Zhang Y, Wong ML, et al. Myocardial infarct size measurement in the mouse chronic infarction model: comparison of area- and length-based approaches. *J Appl Physiol (1985)*. 2007;102:2104–2111.

26. Voorhees AP, DeLeon-Pennell KY, Ma Y, et al. Building a better infarct: modulation of collagen cross-linking to increase infarct stiffness and reduce left ventricular dilation post-myocardial infarction. *J Mol Cell Cardiol*. 2015;85:229–239.

27. Beak JY, Huang W, Parker JS, et al. An oral selective alpha-1A adrenergic receptor agonist prevents doxorubicin cardiotoxicity. *J Am Coll Cardiol Basic Trans Science*. 2017;2(1):39–53.

28. Buerger A, Rozhitskaya O, Sherwood MC, et al. Dilated cardiomyopathy resulting from high-level myocardial expression of Cre-recombinase. *J Card Fail*. 2006;12:392–398.

29. Jensen BC, Swigart PM, Simpson PC. Ten commercial antibodies for alpha-1-adrenergic receptor subtypes are nonspecific. *Naunyn Schmiedebergs Arch Pharmacol*. 2009;379:409–412.

30. Hanna A, Shinde AV, Frangogiannis NG. Validation of diagnostic criteria and histopathological characterization of cardiac rupture in the mouse model of nonreperfused myocardial infarction. *Am J Physiol Heart Circ Physiol*. 2020;319:H948–H964.

31. Gao XM, Xu Q, Kiriazis H, Dart AM, Du XJ. Mouse model of post-infarct ventricular rupture: time course, strain- and gender-dependency, tensile strength, and histopathology. *Cardiovasc Res*. 2005;65:469–477.

32. Li W. Biomechanics of infarcted left ventricle: a review of modelling. *Biomed Eng Lett*. 2020;10: 387–417.

33. Ma Y, Halade GV, Zhang J, et al. Matrix metalloproteinase-28 deletion exacerbates cardiac dysfunction and rupture after myocardial infarction in mice by inhibiting M2 macrophage activation. *Circ Res*. 2013;112:675–688.

34. Matsumura S, Iwanaga S, Mochizuki S, Okamoto H, Ogawa S, Okada Y. Targeted deletion or pharmacological inhibition of MMP-2 prevents cardiac rupture after myocardial infarction in mice. *J Clin Invest*. 2005;115:599–609.

35. Bangert A, Andrassy M, Muller AM, et al. Critical role of RAGE and HMGB1 in inflammatory heart disease. *Proc Natl Acad Sci U S A*. 2016;113: E155–E164.

36. Del Re DP, Amgalan D, Linkermann A, Liu Q, Kitsis RN. Fundamental mechanisms of regulated

cell death and implications for heart disease. *Physiol Rev*. 2019;99:1765–1817.

37. Gupta K, Phan N, Wang Q, Liu B. Necroptosis in cardiovascular disease — a new therapeutic target. *J Mol Cell Cardiol*. 2018;118:26–35.

38. Lindsey ML, Bolli R, Canty JM Jr, et al. Guidelines for experimental models of myocardial ischemia and infarction. *Am J Physiol Heart Circ Physiol*. 2018;314:H812–H838.

39. Zhang T, Zhang Y, Cui M, et al. CaMKII is a RIP3 substrate mediating ischemia- and oxidative stress-induced myocardial necroptosis. *Nat Med*. 2016;22:175–182.

40. Takahashi N, Duprez L, Grootjans S, et al. Necrostatin-1 analogues: critical issues on the specificity, activity and in vivo use in experimental disease models. *Cell Death Dis*. 2012;3:e437.

41. Martin-Sanchez D, Fontecha-Barriuso M, Carrasco S, et al. TWEAK and RIPK1 mediate a second wave of cell death during AKI. *Proc Natl Acad Sci U S A*. 2018;115:4182–4187.

42. Oerlemans MI, Liu J, Arslan F, et al. Inhibition of RIP1-dependent necrosis prevents adverse cardiac remodeling after myocardial ischemia-reperfusion in vivo. *Basic Res Cardiol*. 2012;107: 270.

43. Degterev A, Ofengeim D, Yuan J. Targeting RIPK1 for the treatment of human diseases. *Proc Natl Acad Sci U S A*. 2019;116:9714–9722.

44. ALLHAT Collaborative Research Group. Major cardiovascular events in hypertensive patients randomized to doxazosin vs chlorthalidone: the antihypertensive and lipid-lowering treatment to prevent heart attack trial (ALLHAT). [see comments]. *JAMA*. 2000;283(15):1967–1975.

45. Lusty A, Siemens DR, Tohidi M, Whitehead M, Tranmer J, Nickel JC. Cardiac failure associated with medical therapy of benign prostatic hyperplasia: a population based study. *J Urol*. 2021;205: 1430–1437.

46. Zhao X, Park J, Ho D, et al. Cardiomyocyte overexpression of the alpha1A-adrenergic receptor in the rat phenocopies second but not first window preconditioning. *Am J Physiol Heart Circ Physiol*. 2012;302:H1614–H1624.

47. Kaidonis X, Niu W, Chan AY, et al. Adaptation to exercise-induced stress is not dependent on cardiomyocyte alpha1A-adrenergic receptors. *J Mol Cell Cardiol*. 2021;155:78–87.

48. Gao XM, Ming Z, Su Y, et al. Infarct size and post-infarct inflammation determine the risk of cardiac rupture in mice. *Int J Cardiol*. 2010;143:20–28.

49. Forte E, Skelly DA, Chen M, et al. Dynamic interstitial cell response during myocardial infarction predicts resilience to rupture in genetically diverse mice. *Cell Rep*. 2020;30:3149–3163 e6.

50. Przyklenk K, Connelly CM, McLaughlin RJ, Kloner RA, Apstein CS. Effect of myocyte necrosis on strength, strain, and stiffness of isolated myocardial strips. *Am Heart J*. 1987;114:1349–1359.

51. Shan B, Pan H, Najafov A, Yuan J. Necroptosis in development and diseases. *Genes Dev*. 2018;32: 327–340.

52. Guo X, Yin H, Li L, et al. Cardioprotective role of tumor necrosis factor receptor-associated factor 2 by suppressing apoptosis and necroptosis. *Circulation*. 2017;136:729–742.

53. Zhang H, Yin Y, Liu Y, et al. Necroptosis mediated by impaired autophagy flux contributes to adverse ventricular remodeling after myocardial infarction. *Biochem Pharmacol*. 2020;175: 113915.

54. Schomig A. Adrenergic mechanisms in myocardial infarction: cardiac and systemic catecholamine release. *J Cardiovasc Pharmacol*. 1988;12(suppl 1):S1–S7.

55. Wu P, Cai M, Liu J, Wang X. Catecholamine surges cause cardiomyocyte necroptosis via a RIPK1-RIPK3-dependent pathway in mice. *Front Cardiovasc Med*. 2021;8:740839.

56. Kung G, Konstantinidis K, Kitsis RN. Programmed necrosis, not apoptosis, in the heart. *Circ Res*. 2011;108:1017–1036.

57. Wei JT, Calhoun E, Jacobsen SJ. Urologic diseases in America project: benign prostatic hyperplasia. *J Urol*. 2005;173:1256–1261.

KEY WORDS adrenergic α1 receptor antagonists, myocardial infarction, necroptosis, receptors, adrenergic alpha

---

APPENDIX For supplemental figures and video, please see the online version of this article.